



## Soybean Root Development Relative to Vegetative and Reproductive Phenology

Jessica A. Torrion, Tri D. Setiyono, Kenneth G. Cassman,  
Richard B. Ferguson, Suat Irmak, and James E. Specht\*

### ABSTRACT

Knowledge of soybean [*Glycine max* (L.) Merr.] primary, secondary, and tertiary root tip locations in the soil vs. seasonal time would enhance modeling of soybean development. The seasonal progression of root tip development and shoot phenology was evaluated in situ using an imaging device inserted into minirhizotron tubes installed in the soil at an in-row 30° angle. Primary root tip extension was linear (i.e., 1.5 and 1.2 cm d<sup>-1</sup> each year) until the full-seed stage. Emergent 5-mm secondary roots were routinely detected about 10-cm above the primary root tip, and thus present in a soil layer 11 d after the primary root tip had passed through that layer. Secondary roots followed a similar temporal pattern. Primary root tip location in the soil paralleled a 17°C soil temperature isoline. The 3.7-d phyllochron of main-stem node accrual between first node and seed fill may be a calibratable proxy for inferring correspondent root tip depths.

THE SOYBEAN ROOT system is characterized as diffuse, but has three distinct morphologically defined components: the primary root, commonly called the taproot that originates as the radicle from a germinating seed, the lateral roots, often referred to as secondary roots that emerge from the taproot, and the tertiary roots that originate from lateral roots (Lersten and Carlson, 2004). The primary root is strongly geotropic and typically has a large diameter (Mitchell and Russell, 1971). The maximum rooting depth attained by a soybean root system, which almost invariably is the depth of the primary root tip, and the composite root length density of all three root types at any given soil depth, are affected by soil texture, moisture, and temperature (Glinski and Lipiec, 1990), plus tillage and planting date (Turman et al., 1995).

Detailed quantification of the phenology of root development requires temporally repetitive measurements of root systems during the course of a growing season. Such measurements are difficult to conduct, and the lack of root phenology data is why roots are often referred to as the significant “hidden” but critically important fraction of a plant (Waisel et al., 2002). However, the importance of understanding the synchronicity that may exist between soybean root phenology and soybean vegetative (Vn) and reproductive (Rn) phenology should not be overlooked. A calibration of the root phenology with some aspect of shoot

phenology might be useful, if the latter can serve as a proxy for estimating the likely crop rooting depth on any given growing season day. This predictive capability would substantively improve the reliability of crop simulation models such as SoySim (Setiyono et al., 2010), and irrigation management decision tools such as SoyWater (Specht et al., 2010).

Soybean rooting depth research dates back to the 1970s. Mayaki et al. (1976) evaluated soybean rooting depth over time using a soil core method on irrigated and rainfed fields in Kansas for a maturity group (MG) 3.0 soybean cultivar. Seemingly identical sigmoid growth patterns were observed under both water regimes, with both having logistic model inflection points (i.e., maximum rate) between the beginning bloom (R1) and the full seed (R6) stages. These authors made note of an earlier published report that examined the temporal pattern of primary root depth of a soybean cultivar planted in Iowa using a monolith root observation method (Mitchell and Russell, 1971). These latter authors evaluated composite root lengths in the soil on four seasonal sampling dates of 31, 67, 80, and 102 days after planting (DAP), and stated that these sampling dates demarked the start and end of root growth phases that corresponded to: (i) the vegetative growth phase, (ii) the R1 to beginning pod (R3) early reproductive growth phase, and (iii) the beginning seed (R5) to beginning maturity (R7) late reproductive growth phase. They reported a gradual rate of primary root tip extension during Phase 1 of vegetative growth, a rapid rate of primary root tip extension during Phase 2 of early reproductive growth, and a decreased rate of primary root tip extension, coupled with a downward secondary root proliferation, during Phase 3 of late reproductive development. Kaspar et al. (1978) reported similar

J.A. Torrion, K.G. Cassman, R.B. Ferguson, and J.E. Specht, Agronomy and Horticulture, Univ. of Nebraska-Lincoln, Lincoln, NE 68583-0915; T.D. Setiyono, International Rice Research Institute, DAPO Box 777, Metro Manila, 1301 Philippines; S. Irmak, Biological Systems Engineering, Univ. of Nebraska-Lincoln, P.O. Box 830726 Lincoln, NE 68583-0726. Received 1 June 2012. \*Corresponding author (jspecht1@unl.edu).

Published in *Agron. J.* 104:1702–1709 (2012)

Posted online 17 Sept. 2012

doi:10.2134/agronj2012.0199

Copyright © 2012 by the American Society of Agronomy, 5585 Guilford Road, Madison, WI 53711. All rights reserved. No part of this periodical may be reproduced or transmitted in any form or by any means, electronic or mechanical, including photocopying, recording, or any information storage and retrieval system, without permission in writing from the publisher.

**Abbreviations:** CRD, completely randomized design; DAE, days after emergence; DAP, days after planting; MG, cultivar maturity group; RCB, randomized complete block; RMSE, root mean square error; R1, beginning bloom; R2, full bloom; R3, beginning pod; R4, full pod; R5, beginning seed; R6, full seed; R7, physiological maturity; R8, 95% pod maturity; SoySim, soybean simulation model; SoyWater, a web-based decision tool for soybean irrigation scheduling; V1, first-node; VE, emergence; Vn, vegetative node (where n corresponds to the ordinal number of the given main stem node).

findings on root observations of soybean plants grown in a rhizotron in Ames, IA.

The foregoing reports of seasonally logistic or sigmoid root growth patterns were not confirmed in subsequent research. Mason et al. (1982) found that soybean primary root tip extension rate in an Iowa soil to be linear (i.e., constant) from just after planting to 70 DAP, irrespective of whether soil temperatures at the observed rooting depths were 15°C or warmer. Linear extension of the primary root and secondary roots was reported by Stone and Taylor (1983), based on root data collected using a temperature-controlled water bath with greenhouse-grown plants. These authors stated that at a 17°C soil temperature, the rate of extension of the primary root or secondary roots for all soybean cultivars was constant (i.e., about 2 cm d<sup>-1</sup>), indicating again a linear, rather than logistic, rate that also was insensitive to temperature above 17°C.

Although a minimum soil temperature (i.e., 15°C) has been reported for root activity (Mason et al., 1982), a temporary chilling at 10°C of soybean roots did not affect subsequent root activity at warmer temperatures. However, root chilling impacted shoot growth and development, specifically the leaf elongation rate and subsequent reproductive development (Musser et al., 1983). A controlled-temperature rhizotron study was conducted in Wisconsin by Bland (1993) to evaluate three soybean root growth soil temperature regimes: (i) keeping entire soil column temperature equal to the diurnal changes in air temperature, (ii) simulation of the daily soil temperature rise (16–24°C) per centimeter of depth that nominally occurs after soybean planting in a typical Iowa field, and (iii) simulation of about half the nominally expected daily rate of soil temperature rise per centimeter soil depth. This author reported that primary root tip extension was linear in all three respective temperature regimes, though the magnitude of the linearity was temperature sensitive, given the corresponding regression coefficients of 2.6, 1.2, and 0.9 cm d<sup>-1</sup> from 40 to 120 DAP.

Unlike soybean root growth, soybean shoot phenology (Vn and Rn stages) can be tracked by an observer using the staging system described by Fehr et al. (1971). Those phenological stages could theoretically be used as a proxy to infer contemporaneous root phenology. However, the accuracy and precision of those inferences requires good quality field data for this temporal calibration. Other than the seasonally sparse data provided in the reports just noted, such detailed calibration data are not available especially for modern cultivars now being grown.

Soybean main stem node accrual is substantively linear from the first-node (V1) stage until the Vn stage coincident with the R5 stage. Bastidas et al. (2008) clearly documented a constant phyllochron of 3.7 d (i.e., 0.274 nodes d<sup>-1</sup>) between those two stages, despite the gradual seasonal rise in air temperature between those stages, and irrespective of a 45-d range in planting dates from late April to mid-June in Lincoln, NE. Soybean Vn and Rn phenology can also be forecast by crop simulation models that take into account the air temperature and photoperiod sensitivity of soybean (Major et al., 1975; Boote et al., 1998; Setiyono et al., 2007). That said, the seemingly temperature-insensitive constant node accrual from V1 to Vn at R5 stage reported by Bastidas et al. (2008) would be quite advantageous for making concurrent extrapolative estimates of soybean rooting depth during the V1 to Vn (at R5) stages during

the growing season, assuming that root depth could be calibrated with the coincident Vn stages.

Here we report the results from a 2-yr field experiment with two objectives. The first was to monitor (with frequent temporal sampling) the extension of the soybean primary root tip into soil from seedling emergence to late reproductive development, and to concurrently monitor the depths at which secondary roots incrementally emerged at a point distal from the primary root tip, and also the depths at which tertiary roots incrementally emerged from lateral roots. The second objective was to determine the relationship between shoot Vn and Rn phenology and root system phenology.

## MATERIALS AND METHODS

An indeterminate soybean cultivar (P93M11) was planted on 1 May 2009 and 26 Apr. 2010 at a 3.8-cm planting depth, a seeding rate of 28 seeds m<sup>-1</sup> row (20 plants m<sup>-1</sup> counted at maturity), and a row spacing of 76.2 cm in a field located on the East Campus of the University of Nebraska, Lincoln (40°50'5" N, 96°39'19" W and 357 m above mean sea level). The soil was a Zook silty clay loam of fine, smectitic, mesic Cumulic Vertic Endoaquoll (Soil Survey Staff, 2010). The field was fall plowed after a previous maize (*Zea mays* L.) crop, and then field-cultivated twice in the spring after a herbicide application before planting. In-season weed control was achieved by occasional hoeing during the early vegetative stages. In both years, daily air temperature, and soil temperature in 10-cm section of surface soil under grass vegetation, plus rainfall were recorded at an automated nearby weather station (name: LincolnIANR; www.hprcc.unl.edu) located 500 m from the research field (Table 1).

A minirhizotron approach, employing 1.8-m long translucent acrylic tubes, was used to monitor root growth each year. There are no reports in the literature in which this particular method has been used in soybean root studies. Tubes (with capped bottoms) were inserted into the soil to a depth of 1.2 m, using a truck-mounted hydraulic Giddings probe to first remove a core of soil, and then to gently push the tube into the cored hole. The probe and tubes had an outside diameter of 5.4 cm, thereby providing a snug-fit interface between the tube and the surrounding soil. The tubes were inserted at 30° angle from vertical, with the angle aligned to an in-row direction beneath the plants (Fig. 1). The tube top was sealed with a cap to prevent entry of rain water and kept dark by covering the exposed tube

**Table 1. Mean air and soil temperature and rainfall during the growing season in 2009 and 2010, as recorded at an automated weather station near the experimental field site.**

Variable and year	May	June	July	Aug.	Sept.	Season
	°C					
Temperature, mean						
Air						
2009	17.9	22.3	22.7	22.7	18.4	20.8
2010	16.3	23.6	25.7	26.1	19.4	22.2
Soil, 10 cm						
2009	19.3	23.8	25.8	25.2	20.5	22.9
2010	18.2	25.5	27.7	27.5	21.3	24.0
	mm					
Rainfall, total						
2009	29	137	43	79	93	381
2010	80	264	151	90	116	701

top with a larger diameter (capped) section of polyvinyl chloride opaque pipe.

In 2009, 15 tubes were inserted just after planting at random positions no less than four plant rows apart in a rainfed field site. The experimental set-up was a completely randomized design (CRD) with 15 replications (tubes). In 2010, the experimental design was a randomized complete block (RCB) that included three planned water regime treatments: (a) rainfed, (b) full-season irrigation scheduled by weekly crop evapotranspiration (ET) replacement, and (c) irrigation also scheduled by ET replacement, but with no irrigation before stage R3. These three treatments constituted randomized main plots within each of six replicates. The main plots were 6 m wide and 15 m long. A tube was inserted just after planting into plant row number four in each of the eight-row wide three water treatment main plots present in each of the six replicates.

Root depth data were collected each year with an imaging camera inserted into the acrylic tubes twice per week (weather permitting), starting at about emergence (VE) and continuing until the plant roots reached the tube bottom, so the maximum rooting observation depth was 1.2 m. Two imaging cameras were used: a BTC100X Minirhizotron Video Microscope ([\[bartztechnology.com/\]\(http://bartztechnology.com/\)\) in 2009 and a CI-600 Root Scanner \(<http://www.cid-inc.com/ci-600.php>\) in 2010. Shifting to the CI-600 root scanner in 2010 permitted more comprehensive imaging data, and more importantly enabled the imaging to be conducted more quickly, allowing the operator to complete the imaging in all 18 tubes in a single day. In addition, soil excavation pits were dug on occasional dates in 2010 \(in the available rows of the rainfed treatment\) to acquire direct observational root data from a sample of five plants carefully removed from the side walls of the excavation pit.](http://</a></p>
</div>
<div data-bbox=)

Rooting depths were derived from the imaging data using the software programs known as Rootfly (Birtchfield and Wells, 2011) and Image Tool (Wilcox et al., 2002) for the respective 2009 BTC100X and 2010 CI-600 cameras. Rootfly was custom-built for the BTC100X image file format, and thus could not be used with the CI-600 image file format. Because of the within-row 30° angling of the acrylic tubes, the downwardly extending taproot tips of the plants growing in the rows were expected to progressively come into contact with the angled acrylic tube at successive seasonal sampling dates, as shown diagrammatically in Fig. 1 (i.e., panels A and B). Because a tube for which a taproot tip was just touching it on a given imaging date, may not have shown a *new* taproot tip just touching it at the next imaging date, on most sampling dates, only about half of the tubes imaged a given day provided *new* taproot tip depth data.

Taproot tips just touching the acrylic tube on a given imaging day (Fig. 1) were assigned an imaging root depth value that was adjusted to obtain actual root depth using the equation:  $RD = iRD \times (\cos\theta)$ , where RD is the rooting depth, *iRD* is the imaged rooting depth (obtained with either the BTC100X or CI-600 camera), and  $\theta$  is tube angle. As the taproot tip extended into the soil, lateral roots emerged from the taproot at points distal from the taproot tip. The emerging lateral roots of camera imaging interest were those that elongated to a length (i.e., 5 mm) that allowed certainty in calling the protuberances newly emergent lateral roots. The soil depth when such 5-mm long secondary roots were visible was recorded on each imaging date (Fig. 1). A similar criterion was used to record the date and depth of the first 2-mm long tertiary roots to emerge from lateral roots. When plant root systems were directly observed by careful removal of soil from the excavated pit sidewalls, the same 5-mm criterion for lateral root emergence from the taproot was used. However, because tertiary roots could not be reliably observed in the excavation pit sidewalls, no data on these were collected in the excavation pits.

Soybean shoot phenological stages were scored twice per week in each year, as described by Fehr and Caviness (1977), using a contiguous sample of 20 plants in a randomly selected section in each of two rows near the acrylic tubes (i.e., 40 total plants examined). Heights of the plants in those sections, measured from ground level to main stem tips, were also recorded on each scoring date.

Because taproot extension into the soil, and emergence of lateral roots from the taproot, plus the emergence of tertiary roots from the lateral roots vs. sampled days after emergence (DAE) appeared to be linear in each year, those measurements were modeled using a linear regression model,  $y = bx + a$ , where *y* was soil depth, *x* was DAE, *b* was the regression coefficient, and *a* was the *y* intercept when *x* = 0.

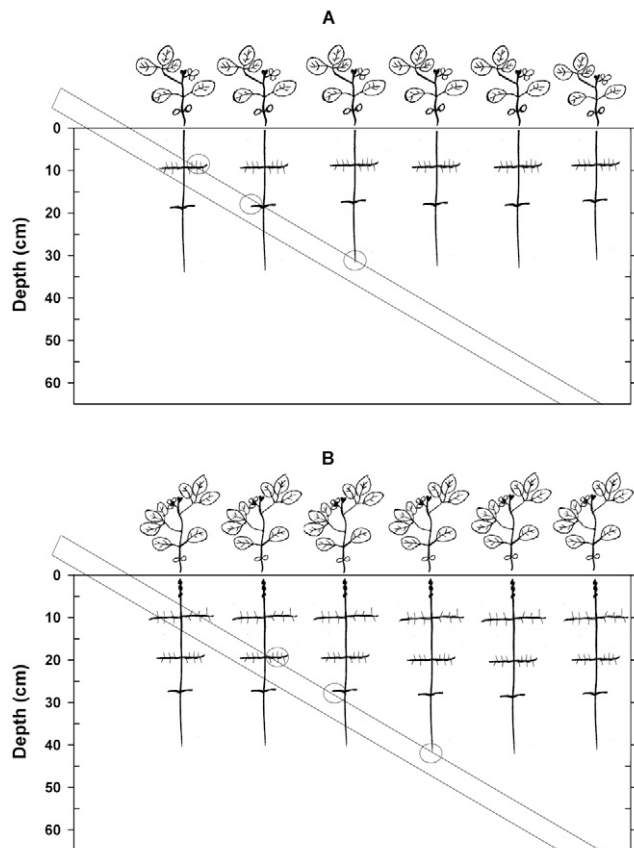


**Fig. 1.** An illustration of a single minirhizotron acrylic tube installed in the field in the row at a 30° angle. Plant roots are hypothetically shown in that row extending downward on sampling dates of 23 days after emergence (DAE) at a second-node (V2) stage in panel A, and at 27 DAE at a third-node stage (V3) in panel B. The 4-d differential between the two panels depicts the intersection of the plant root system with the acrylic tube over time, and thus how the camera, when inserted into the tube, could capture images of the primary root (taproot) tip, secondary roots, and tertiary roots as the growing roots progressively encountered lower portions of the acrylic tube.

Main stem node accrual observations recorded during shoot Vn phenology were fit to a tri-phasic linear pattern as described by Bastidas et al. (2008), wherein the vegetative main stem node  $y$ -axis values were scaled from an initial value of  $-2$  to a final main stem node  $n$ , thereby allowing the inclusion of planting date and emergence events in the  $y$ -axis scale. Thus, the “vegetative state” on the date of planting was assigned a  $y$ -axis Vn “node” value of V-2, stage VE (emergence) was assigned a  $y$ -axis Vn “node” value of V-1, stage V0 (cotyledon node) was assigned a  $y$ -axis value of zero, and subsequent Vn nodes were assigned their respective  $n$  ordinal numbers of 1 on up to the final main stem node  $n$  in each year. Rn stages are not linear with time (Bastidas et al., 2008), so Rn stage values were depicted in the graphs as ordinal Rn points connected by a dotted line (i.e., the latter is provided for visual interpolative purposes).

Seasonal stem height data were fitted with a 3-parameter logistic function,  $Y = A/1 + \exp[-(X - X_0)/B]$ , where  $Y$  was stem height,  $X$  was DAE,  $A$  represented the maximum stem height achieved each year,  $X_0$  was the logistic inflection point, and  $B$  was the logistic coefficient.

Variation in soil temperature with depth and time was simulated using the thermodynamic heat flux of a specific soil to estimate temperature at any depth as described by Hillel (1982), and modeled by Nofziger and Wu (2005), using a thermal diffusivity of the field site soil texture, minimum and maximum soil surface temperature, and the Julian day of the year (DOY) occurrence of minimum soil temperature. The degree of congruence between the simulated soil temperatures and the observed soil temperatures (recorded at the nearby weather station) was evaluated by the root mean square error (RMSE) method described by Janssen and Heuberger (1995), and calculated as:

$$\text{RMSE} = \sqrt{\frac{\sum (s_i - o_i)^2}{n}}$$

where  $s$  is the simulated temperature,  $o$  is the weather station recorded soil temperature, both on the  $i$ th day, and  $n$  is the  $d$  of 365-d year. Finally, in each year, soil temperature isolines of 13, 15, 17, and 20°C, as per Nofziger and Wu (2005) soil temperature simulation were plotted along with the seasonal rooting depth pattern.

## RESULTS AND DISCUSSION

Seasonal air temperature and precipitation patterns differed between 2009 and 2010 (Table 1). The 2010 season was generally warmer and exhibited a month-to-month air temperature rise of 7.0, 2.1, and 0.4°C from May to June, June to July, and July to August, respectively. In 2009, May was warmer and the corresponding month-to-month air temperature rises were smaller (4.4, 0.4, and 0.0°C). The seasonal soil temperature, measured at the weather station (10-cm depth, grass vegetation), also was warmer in 2010, except in May.

Total seasonal precipitation was greater in 2010, though August rainfall was similar in both years (Table 1). The near-double precipitation amounts received during May, June, and July in 2010 essentially negated our plan to evaluate rooting depth in three planned water treatment main plots in each of the six replicates, because irrigation was not needed until after the

observed taproot tip reached the maximum depth of observation (i.e., 1.2 m). For that reason, the 2010 data presented herein were combined over the three main water treatment plots.

One of our objectives was to monitor shoot growth and development while concurrently tracking root growth and development. Let us first consider the shoot phenology data.

The seasonal change in main stem height in 2009 and 2010 followed a sigmoidal pattern, and was modeled with a 3-parameter logistic function (Fig. 2A, 3A). The acceleration and deceleration phases of the logistic patterns did not overtly differ much between years, though the logistic parameters did differ numerically. The 2009 main stem growth accelerated slightly faster from V1 to a 49-DAE inflection point coinciding with the full-bloom (R2) stage, then decelerated to a plateau shortly after the plants attained stage R5. In 2010, the acceleration was slightly slower and the 54-DAE inflection point occurred somewhat later, between stages R2 and R3. The seasonal change in main stem length is mostly attributable to successive lengthening of each internode, though the number of main stem nodes does determine the number of internodes. Internode length is sensitive to coincident air temperature (Bastidas et al., 2008), so the more rapid 2009 acceleration in stem height was likely due to the warmer May air temperatures that year (Table 1), which resulted in longer (early formed) internode lengths. However, the warmer temperatures in June and July of 2010 led to longer (later formed) internodes, resulting in taller mature plants that year, which is evident in the logistic A parameter values of 107 ( $\pm 3.5$ ) cm in 2009 and 117 ( $\pm 3.6$ ) cm in 2010 (Fig. 2A, 3A).

The main stem node accrual rates in each year were nearly identical both years (Fig. 2B, 3B), and were linear from V1 to the Vn coinciding with stage R5. The linear rates of 0.27 node  $d^{-1}$  in 2009 (before it ceased at V17), and 0.28 node  $d^{-1}$  in 2010 (before it ceased at V17.5) were very close to the node accrual rate of 0.274 node  $d^{-1}$  reported by Bastidas et al. (2008) for multiple planting dates in 2003 and 2004. These data and those of Bastidas et al. (2008) indicate that main stem node accrual from V1 to R5 is relatively constant despite variation in seasonal air temperatures, which would make temperature-insensitive Vn stage phenology a useful proxy for coincident inference of root development, assuming that rooting status can be calibrated to the linearity of Vn node occurrence.

Reproductive stages R1, full-pod stage (R4), and R5 occurred at near-identical DAEs in each year (Fig. 2B, 3B). However, stages R2, R3, and R6 were 3, 10, and 4 d earlier in 2010. A biological explanation for the earliness of the foregoing three R stages is not obvious, though the duration of each post-flowering stage (from R1–R7) is known to be influenced by the coincident air temperatures (Setiyono et al. 2007), and 2010 was warmer during those reproductive stages in July and August (Table 1).

It is important to recognize that stage R5 did occur on a similar date in each year, and shortly after its occurrence, the development of new nodes at the main stem apex abruptly slowed down (Fig. 2B, 3B). Bastidas et al. (2008) noted the same phenomenon and stated that this was because newly developing seeds were becoming a strong photosynthetic sink at R5, diverting photosynthate from vegetative stem tip meristematic growth (Sinclair, 1984; Setiyono et al., 2007; Bastidas et al., 2008).

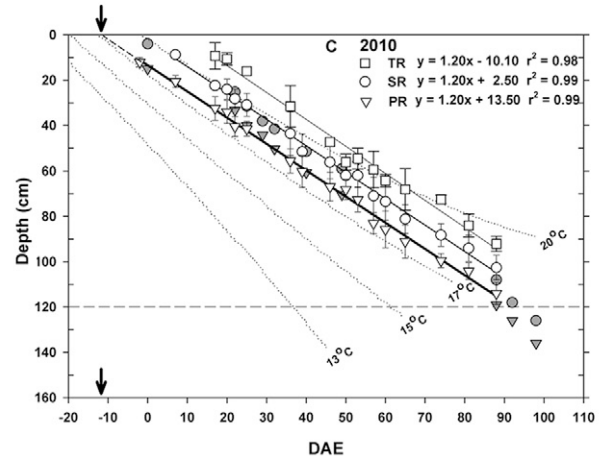
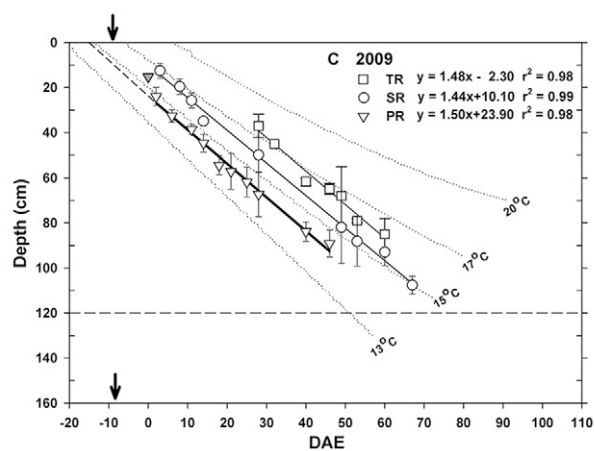
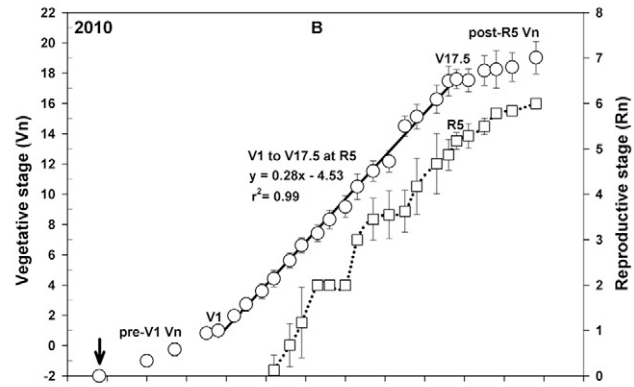
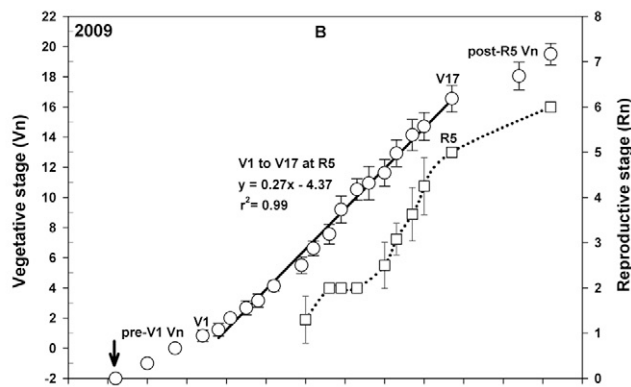
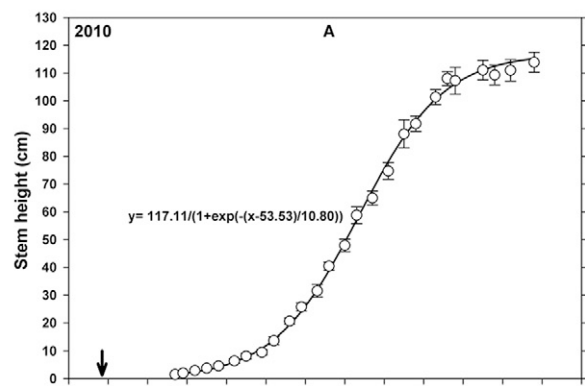
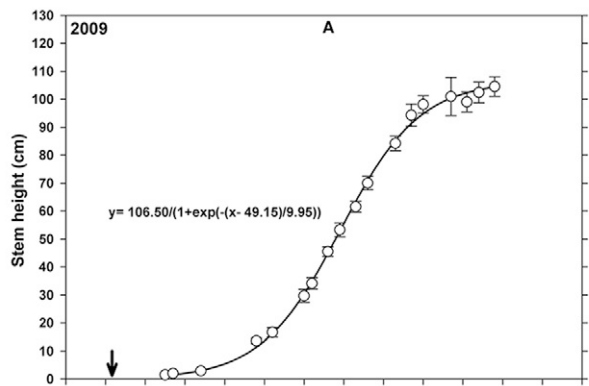


**Fig. 2.** Graphs of 2009 means and model equations for main stem height (panel A), vegetative (Vn) stage (left axis) and reproductive (Rn) stage (right axis) development (panel B), and soil depth (left axis) of the primary root tip, newly emerged secondary root, and newly emerged tertiary root systems (panel C) vs. days after emergence (DAE). The downward pointing arrows indicate the planting date in DAE terms. The solid symbols in panel C represent plant primary and secondary root systems obtained by soil excavation. In panel A, a logistic model was fit to the data. In panel B, a triphasic linear model was used for the (1) pre-V1 phase, (2) post-V1 to V17 phase (i.e., V17 was coincident with R5), and (3) post-R5 Vn phase. For clarity, only the regression equation for the central phase is shown. The dotted line of the R-stage is not a modeled representation of R-stage occurrence vs. DAE, but simply connects the Rn stages that were called on the given DAE. In panel C, the dotted lines denote depths of the soil thermal isolines of 13, 15, 17, and 20°C vs. DAE. Observation numbers for the means were  $n = 20$  for the stem height in panel A,  $n = 40$  for V stage and R stage in panel B, and  $n = 5$  to 7 for the primary, secondary, and tertiary roots in panel C.

**Fig. 3.** Graphs of 2010 means and model equations for main stem height (panel A), vegetative (Vn) stage (left axis) and reproductive (Rn) stage (right axis) development (panel B), and soil depth (left axis) of the primary root tip, newly emerged secondary root, and newly emerged tertiary root systems (panel C) vs. days after emergence (DAE). The downward pointing arrows indicate the planting date in DAE terms. The solid symbols in panel C represent plant primary and secondary root systems obtained by soil excavation. In panel A, a logistic model was fit to the data. In panel B, a triphasic linear model was used for the (1) pre-V1 phase, (2) post-V1 to V17 phase (i.e., V17 was coincident with R5), and (3) post-R5 Vn phase. For clarity, only the regression equation for the central phase is shown. The dotted line of the R-stage is not a modeled representation of R-stage occurrence vs. DAE, but simply connects the Rn stages that were called on the given DAE. In panel C, the dotted lines denote depths of the soil thermal isolines of 13, 15, 17, and 20°C vs. DAE. Observation numbers for the means were  $n = 20$  for the stem height in panel A,  $n = 40$  for V stage and R stage in panel B, and  $n = 5$  to 13 for the primary, secondary, and tertiary roots in panel C.

The data of relevance to our main objective is presented in Fig. 2 (2009) and Fig. 3 (2010), where the C panels depict the seasonal patterns of root development corresponding to not only the coincident seasonal patterns of increasing plant height depicted in the A panels, but also the successive stages of shoot growth and reproductive development presented in B panels. In 2009, taproot tip extension into the soil vs. time was linear, moving downward at a constant rate of  $1.50 \text{ cm d}^{-1}$  ( $r^2 = 0.99$ ) during span of 2 to 48 DAE, for which there were 10 sampling dates (Fig. 2C). Extrapolation of the regression line back to DAE = 0 generated a  $y$  intercept of 23.90 cm, which is a speculative projection of the presumed seedling radical root tip depth at stage VE. Using a shovel that year to excavate some seedlings on the date of VE, the in situ VE seedling radical root tip was determined to be 15.3 cm (Fig. 2C, solid triangle symbol). The 8.6-cm root tip depth differential between the camera-imaged tip depth observations and the tip depth directly observed on excavation was thought at time to be experimental error associated with first-year camera images taken by an inexperienced operator. With the experience gained after the first year, a new camera allowing almost twice as many sampling dates, and with the digging of excavation pits at various seasonal time-points in 2010 to conduct direct root system observations, there was more confidence in the second year of camera imaged data. The taproot tip extension was again linear in 2010 (Fig. 3C), and when averaged over the three main plots and six replicates, was  $1.20 \text{ cm d}^{-1}$  ( $r^2 = 0.99$ ), which was lower than the  $1.50 \text{ cm d}^{-1}$  rate less confidently measured in 2009. The 2010 DAE = 0  $y$  intercept of 13.50 cm was not substantively different from a soil-excavated seedling radicle tip depth of 15 cm (Fig. 3C; upper left solid triangle symbol). Moreover, there was a strong correspondence between the camera-imaged taproot tip data and excavation-based directly observed taproot tip data during the 0- to 85-d span of seasonal observations (Fig. 3C; open vs. solid triangle symbols). Of particular interest was the extrapolation of the 2010 taproot tip regression line backward in time to a  $y$  intercept of  $-8.0$  DAE soil depth of 3.8 cm (seeding depth), which is the speculated date at which the radicle was assumed to have just started to extend into the soil, about 4 d after date of planting of  $-12$  DAE.

In the present study, the taproot tip depth was at 90 cm at 68 DAE (= 80 DAP) in 2010 (Fig. 3C), which was consistent with a similarly observed depth range of detected root dry mass reported at 80 DAP in Iowa by Mitchell and Russell (1971). In the present study, at 88 DAE (= 100 DAP) and just before the R6 stage, the taproot tip depth was 117 cm, which was also consistent with the Iowa data showing the presence of roots at depth of 122 cm at 102 DAP. The 2009 taproot tip depths were somewhat deeper than the 2010 root data (and deeper than the depth data available in the literature) probably because, as already noted, of operator inexperience with the 2009 camera.

The linear rates of taproot tip extension for 2009 and 2010 did not show any apparent curvature change suggestive of a taproot tip extension slow-down or a cessation plateau, at least up to the maximum depth of observation that was possible with the tube lengths in this study (Fig. 2C, 3C). During the seed-fill period (R5 to R6+), the taproot tip still continued to extend linearly into the soil, even though the plants connected to these roots were well into the post-R5 stage. In fact, root system data

collected from excavation pits near the R6 stage (Fig. 3C; solid symbol at 98 DAE) indicated that roots were actually somewhat deeper than what was expected based on an extrapolation of the camera image regression line. The lack of an observable decline in the rate of taproot tip extension in the present study contrasts with the 40-yr-old reports of a declining taproot tip extension rate from R5 to R7 (Mitchell and Russell, 1971; Mayaki et al., 1976). Because no further observations were made after the R6 stage on root extension in the soil at this Nebraska research site (Fig. 3C), it cannot be determined if taproot tip extension did eventually slow or cease, though a cessation of taproot tip extension would obviously be expected to occur at soybean stage R7 (i.e., physiological maturity). Although main stem node accrual ceased in soybean plants that attained R5 stage—a likely result of developing seeds becoming a strong sink for photosynthate (Bastidas et al., 2008), the attainment of R5 in the present study did not seem to impact the extension of the taproot tip (i.e., panels B vs. C in Fig. 2 and 3).

On average, the first detectable emerging 5-mm long secondary roots were observed about 10 cm behind the concurrent depth of the taproot tip (Fig. 2C, 3C). The parallelism of the trend lines for taproot tip depth and depth of the emergent secondary roots suggests that their origination from the taproot operates on a chronological time basis, which can be observed by drawing a horizontal line from any given depth on the  $y$  axis and noting the constant 11-d time differential in 2010 between the taproot and secondary root emergence regression trend lines (i.e., both have a numerically identical regression coefficient). This 11-d differential is an arbitrary one, of course, and would be smaller (or larger) if a secondary root length criterion smaller (or larger) than 5 mm had been chosen for calling a given secondary root as being emerged. Still, this arbitrary criterion does not detract from the clear evidence of the chronological constancy of secondary root emergence from the taproot at some constant position behind the taproot tip (irrespective of the actual seasonal depth of that taproot tip). A recent finding by Moreno-Risueno et al. (2010) reported that root branching in mouse-ear cress [*Arabidopsis thaliana* (L.) Heynh.] exhibited a temporal cycling pattern and that the distal location of secondary root origin behind the taproot tip was predetermined and governed by an endogenous clock mechanism. This report seems to provide an explanation of the constancy of secondary root emergence behind a soybean taproot, but whether the distal position of secondary root emergence in a soybean taproot is endogenously clock-driven will require further research.

Tracking the circumferential emergence of tertiary roots from laterally oriented secondary (lateral) roots that had just emerged from vertically oriented taproots was, in the present study, more difficult than tracking lateral roots per se. This is obvious in Fig. 2C and 3C, for which there are missing tertiary data points on some sampling days, and variability among the standard error bar lengths for those data points. In 2009, collection of tertiary root data was not initiated until later sampling dates due to operator inexperience that year, whereas the 2010 root data collection was conducted with better operator confidence. In 2010, 2-mm long tertiary roots were observed emerging from lateral roots after these lateral roots had extended about 10 cm from their origin on the taproot. Time-wise, the differential was 12.4 d, but

again, this interval is arbitrary, due to the use of a 2-mm length criterion for calling a tertiary root as emerged. It would appear that tertiary roots also emerge from secondary roots in some sort of constant distance and time from the taproot tip, but the data on tertiary root emergence in the present study are more limited than the data on secondary root emergence. Tertiary root emergence from secondary roots should be studied in more detail given that an angling downward of secondary roots emanating from the taproot has been reported to be temperature sensitive (Kaspar et al. 1981; Nagel et al., 2009).

Soil temperature data in a 10-cm depth soil was available from the weather station near the study site, and those shallow soil temperature data are presented in Fig. 4, panels A (2009) and B (2010). Also graphed are the simulated soil temperatures for the soil texture at the experimental site as per the methods described by Nofziger and Wu (2005) for other soil depths. The simulated seasonal soil temperatures at 10-cm below the soil surface and the weather station-reported soil temperatures corresponding to 10-cm depth were in close agreement, as is evident from the RMSE value of only 2.3°C in both years. The simulated soil temperature values were 15 and 17°C just after planting (indicated by the thick arrows in the graphs) in 2009 and 2010, respectively (Fig. 4A, 4B), and this 2°C differential also was

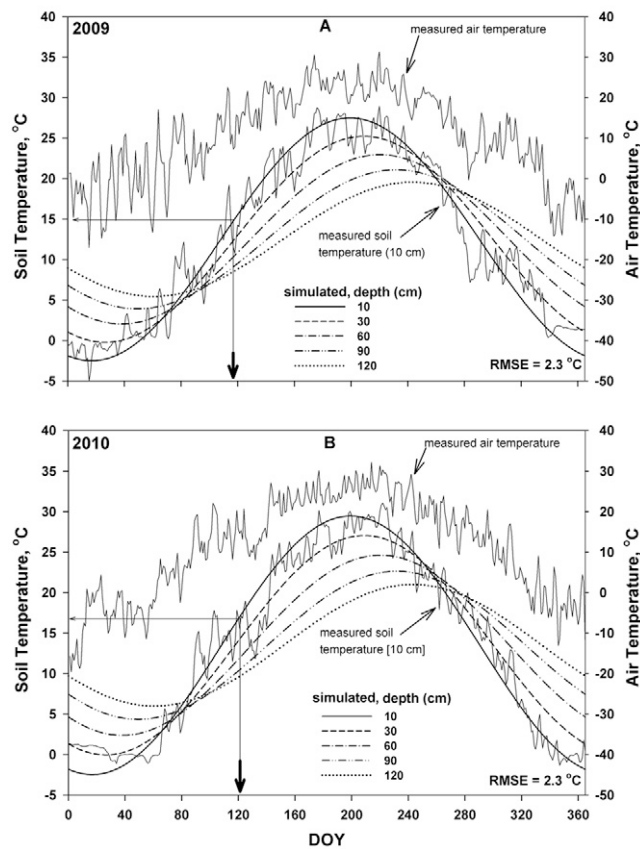


**Fig. 4.** Graphs of 2009 (panel A) and 2010 (panel B) observed air temperatures (right y axis), observed soil temperatures (left y axis) measured at 10 cm at a High Plains Regional Climate Center (HPRCC) station located near the study site, and the simulated soil temperatures at 10-, 30-, 60-, 90-, and 120-cm depths vs. Julian day of the year (DOY). The root mean square error (RMSE) value is presented for the comparison of the 10-cm depth simulated daily soil temperature vs. the 10-cm depth recorded daily soil temperature at the nearby weather station. The arrows indicate the planting date.

evident at the temperature peak at a DOY of 200. Simulation of soil temperature in deeper depths—without corresponding measurement data—is of course somewhat speculative, although Nofziger and Wu (2005) stated that the soil temperature simulation model predicted soil temperature very well over varying depths.

To relate seasonal soil temperatures at five depths in each year with seasonally coincident root depth, the soil temperature isolines shown in Fig. 4 are graphed in Fig. 2C and 3C (dotted lines). The concept of relating soil temperature isolines to rooting growth rate was first suggested by Mason et al. (1982), who observed taproot tip depths between two temperature isolines: 15 and 17°C. In 2009 of the present study, the taproot tip extension regression line was near the 15°C isoline most of the season, whereas in 2010, the taproot tip trend line was near the 17°C isoline most of the season. Assuming that a commonly observed taproot tip depth in field conditions occurs within the 15 to 17°C isolines (Mason et al., 1982), both the 2009 and 2010 imaged root depth data are in agreement with that assumption. However, as noted earlier, there is less confidence in the 2009 images due to operator inexperience in camera imaging. The 2010 taproot tip extension rate was consistent with results reported in the literature with field-grown soybean plants (Bland, 1993; Stone and Taylor, 1983).

Because of the consistent 10-cm distance of SR origination from the taproot tip (Fig. 2C and 3C), it would appear that timing of SR origination from the taproot is not sensitive to temperature. As Nagel et al. (2009) reported, SR growth in spring oilseed rape (*Brassica napus* L.), which has a taproot system similar to that of soybean, was insensitive to temperature. In fact, findings by Stone and Taylor (1983) have shown that the number of SRs emerging from the taproot remained the same at various temperatures.

## SUMMARY

Using main stem height as a parameter to infer taproot depths is unlikely to be reliable because main stem height is a reflection of the summed main stem internode lengths, which Bastidas et al. (2008) noted were influenced by the rise in air temperature from the early spring to mid-summer, and later (at the inception of stage R5) by seed demand for photosynthate. Although stem height is seemingly projectable with a logistic model, not knowing a priori numerical values to use for the logistic *A* parameter (i.e., final stem height) makes actual in-season stem height projection difficult, at least from a proxy standpoint. Despite demonstrating a relationship between stem height and rooting depth by Mayaki et al. (1976), within irrigated and rainfed soybean, there was a considerable stem height difference between these two production systems. Moreover, differences in air temperature and the timing and amount of seasonal rainfall between years also would likely result in unpredictable differences in plant heights.

The constancy of a 3.7-d phyllochron (V1 to stage Vn at stage R5), irrespective of planting date, cultivar, and year (Bastidas et al., 2008)—a phenomenon also confirmed this study, coupled with the linearity of root extension within a 15 to 17°C soil temperature isoline, indicates that main stem node count would be a useful temperature-insensitive shoot parameter to serve as a calibratable proxy for inferring the corresponding rooting depth,

at least during the V1 to R5 period. While Bastidas et al. (2008) reported that the pre-V1 stages were soil, then air, temperature-sensitive; the linearity of taproot tip extension in this study seems to be insensitive. However, additional years and sites of seasonal root parameter data collection will be needed to determine if a seasonal main stem node count can be used as a reliable proxy of the concurrent depth of taproot tips, and emergent lateral roots in the deep well-drained fertile soils common in much of Nebraska and surrounding states.

## REFERENCES

- Bastidas, A.M., T.D. Setiyono, A. Dobermann, K.G. Cassman, R.W. Elmore, G.L. Graef, and J.E. Specht. 2008. Soybean sowing date: The vegetative, reproductive, and agronomic impacts. *Crop Sci.* 48(2):727–740. doi:10.2135/cropsci2006.05.0292
- Birtchfield, S.T., and C.E. Wells. 2011. Rootfly: Software for minirhizotrone image analysis. Clemson Univ, Clemson, SC. <http://www.ces.clemson.edu/~stb/rootfly/> (accessed 1 July 2009).
- Bland, W.L. 1993. Cotton and soybean root system growth in three soil temperature regimes. *Agron. J.* 85(4):906–911. doi:10.2134/agronj1993.00021962008500040023x
- Boote, K.J., J.W. Jones, and G.W. Hoogenboom. 1998. Simulation of crop growth: Cropgro model. In: R.M. Peart and R.B. Curry, editors, *Agricultural systems modeling and simulation*. Marcel Dekker, New York. p. 651–692.
- Fehr, W.R., and C.E. Caviness. 1977. Stages of soybean development. *Spec. Rep. 80. Iowa Agric. Home Econ. Exp. Stn. Iowa State Univ., Ames.*
- Fehr, W.R., C.E. Caviness, D.T. Burmood, and J.S. Pennington. 1971. Stage of development descriptions for soybeans, *Glycine max* (L.) Merrill. *Crop Sci.* 11(6):929–931.
- Glinski, J., and J. Lipiec. 1990. *Soil physical conditions and plant roots*. CRC Press, Boca Raton, FL.
- Hillel, D. 1982. *Introduction to soil physics*. Academic Press, San Diego, CA.
- Janssen, P.H.M., and P.S.C. Heuberger. 1995. Calibration of process-oriented models. *Ecol. Modell.* 83(1–2):55–66. doi:10.1016/0304-3800(95)00084-9
- Kaspar, T.C., C.D. Stanley, and H.M. Taylor. 1978. Soybean root growth during the reproductive stages of development. *Agron. J.* 70(6):1105–1107. doi:10.2134/agronj1978.00021962007000060051x
- Kaspar, T.C., D.G. Woolley, and H.M. Taylor. 1981. Temperature effect on the inclination of lateral roots of soybeans. *Agron. J.* 73(2):383–385. doi:10.2134/agronj1981.00021962007300020034x
- Lersten, N.S., and J.B. Carlson. 2004. Vegetative morphology. In: H.R. Boerma and J.E. Specht, editors, *Soybeans: Improvement, production and uses*. ASA, CSSA, and SSSA, Madison, WI. p. 15–57.
- Major, D.J., D.R. Johnson, J.W. Tanner, and I.C. Anderson. 1975. Effects of daylength and temperature on soybean development I. *Crop Sci.* 15(2):174–179. doi:10.2135/cropsci1975.0011183X001500020009x
- Mason, W.K., H.R. Rowse, A.T.P. Bennie, T.C. Kaspar, and H.M. Taylor. 1982. Responses of soybeans to two row spacings and two soil water levels. II. Water use, root growth and plant water status. *Field Crops Res.* 5:15–29. doi:10.1016/0378-4290(82)90003-x
- Mayaki, W.C., I.D. Teare, and L.R. Stone. 1976. Top and root growth of irrigated and nonirrigated soybeans. *Crop Sci.* 16(1):92–94. doi:10.2135/cropsci1976.0011183X001600010023x
- Mitchell, R.L., and W.J. Russell. 1971. Root development and rooting patterns of soybean (*Glycine max* (L.) Merrill) evaluated under field conditions. *Agron. J.* 63(2):313–316. doi:10.2134/agronj1971.0002196200630002034x
- Moreno-Risueno, M.A., J.M. Van Norman, A. Moreno, J. Zhang, S.E. Ahnert, and P.N. Benfey. 2010. Oscillating gene expression determines competence for periodic arabidopsis root branching. *Science* (Washington, DC) 329(5997):1306–1311. doi:10.1126/science.1191937
- Musser, R.L., S.A. Thomas, and P.J. Kramer. 1983. Short and long term effects of root and shoot chilling of ransom soybean. *Plant Physiol.* 73(3):778–783. doi:10.1104/pp.73.3.778
- Nagel, K.A., B. Kastenholz, S. Jahnke, D. van Dusschoten, T. Aach, M. Mühlich et al. 2009. Temperature responses of roots: Impact on growth, root system architecture and implications for phenotyping. *Funct. Plant Biol.* 36(11):947–959. doi:10.1071/FP09184
- Nofziger, D.L., and J. Wu. 2005. Soil temperature with time and depth. Oklahoma State Univ., Stillwater. <http://soilphysics.okstate.edu/software/Soil-Temperature/> (accessed 12 Jan 2012).
- Setiyono, T.D., K.G. Cassman, J.E. Specht, A. Dobermann, A. Weiss, H.S. Yang et al. 2010. Simulation of soybean growth and yield in near-optimal growth conditions. *Field Crops Res.* 119(1):161–174. doi:10.1016/j.fcr.2010.07.007
- Setiyono, T.D., A. Weiss, J. Specht, A.M. Bastidas, K.G. Cassman, and A. Dobermann. 2007. Understanding and modeling the effect of temperature and daylength on soybean phenology under high-yield conditions. *Field Crops Res.* 100(2–3):257–271. doi:10.1016/j.fcr.2006.07.011
- Sinclair, T.R. 1984. Cessation of leaf emergence in indeterminate soybeans. *Crop Sci.* 24:483–486. doi:10.2135/cropsci1984.0011183X002400030012x
- Soil Survey Staff. 2010. Custom soil resource report. Natural Res. Conserv. Serv., USDA, Washington, DC. <http://websoilsurvey.nrcs.usda.gov/app/HomePage.htm> (accessed 10 Aug. 2009).
- Specht, J.E., J.A. Torrión, T.D. Setiyono, K.G. Cassman, I. Suat, K. Hubbard et al. 2010. Station-specific weather and crop water use: A decision-aid webpage to schedule irrigation in soybeans. Univ. of Nebraska, Lincoln. <http://www.hprcc3.unl.edu/soywater/> (accessed 15 Jan. 2012).
- Stone, J.A., and H.M. Taylor. 1983. Temperature and the development of the taproot and lateral roots of four indeterminate soybean cultivars. *Agron. J.* 75(4):613–618. doi:10.2134/agronj1983.00021962007500040010x
- Turman, P.C., W.J. Wiebold, J.A. Wrather, and P.W. Tracy. 1995. Effect of planting date and tillage system on soybean root growth. *J. Plant Nutr.* 18(12):2579–2594. doi:10.1080/01904169509365086
- Waisel, Y., A. Eshel, and U. Kafkafi. 2002. *Plant roots the hidden half*. 3rd ed. Marcel Dekker, New York.
- Wilcox, D., B. Dove, D. McDavid, and D. Greer. 2002. Univ of Texas Health Sciences Center image tool for windows. Univ. of Texas Health Sci. Ctr., San Antonio. <http://compdent.uthscsa.edu/dig/itdesc.html> (accessed 10 July 2010).